

Is it $SU(2)_L$ or just $U(1)_Y$? 750 GeV di-photon probes of the electroweak nature of new states

Jose Miguel No¹

¹*Department of Physics and Astronomy, University of Sussex, Brighton BN1 9QH, United Kingdom*
(Dated: May 20, 2016)

The existence of a 750 GeV di-photon spin-0 resonance S would imply the additional presence of new particles beyond the Standard Model, coupling directly to S and electromagnetically charged. For an $SU(2)_L$ singlet S , we explore the possibility of probing the $SU(2)_L$ and $U(1)_Y$ quantum numbers of the new states at the LHC by measuring/constraining the WW , $Z\gamma$ and ZZ decays of S . We obtain robust prospects on the required LHC integrated luminosity to discover the new decay modes of S , and discuss the implications of these measurements for probing the electroweak nature of the new states. We also discuss the impact of S mixing with the SM Higgs in such probes.

I. INTRODUCTION

Recently ATLAS [1, 2] and CMS [3, 4] collaborations have observed a large excess in the di-photon spectrum around $m_{\gamma\gamma} \sim 750$ GeV, arising in LHC Run 2 data of pp collisions with center of mass energy $\sqrt{s} = 13$ TeV. This excess strongly points towards the existence of a new neutral particle S with mass $m_S \sim 750$ GeV, and such possibility has since been the subject of an intense research effort, particularly under the assumption of a spin-0 resonance.

Being neutral, the new particle S can only couple to photons via a loop of charged particles. These cannot be Standard Model (SM) particles, since in such case the ratio of decay widths of S into two such SM particles and into two photons would greatly suppress the di-photon decay mode, rendering it unobservable at the LHC (see *e.g.* [5, 6]). This implies the existence of new electromagnetically charged particles χ beyond the SM, with masses $m_\chi \gtrsim 375$ GeV in order to forbid the decay of S into these states. While the properties of these new χ particles may be constrained indirectly, *e.g.* via the measurement of running electroweak (EW) couplings at the LHC [7, 8], a more direct probe would be ultimately required to establish their connection to the 750 GeV resonance phenomenology.

Due to $SU(2)_L \times U(1)_Y$ gauge invariance, the existence of the decay $S \rightarrow \gamma\gamma$ mediated by a loop of χ states automatically implies the existence of other decay modes [9], namely $S \rightarrow Z\gamma$ and $S \rightarrow ZZ$, and also $S \rightarrow WW$ if χ transform non-trivially under $SU(2)_L$. Thus, measuring/constraining the various ratios of branching fractions $R_{VV} \equiv \text{BR}(S \rightarrow VV)/\text{BR}(S \rightarrow \gamma\gamma)$ (with $VV = WW, ZZ, Z\gamma$) could yield valuable information on the $SU(2)_L$ and $U(1)_Y$ quantum numbers of the new states χ mediating the decays of S .

This paper is organized as follows: In Section II we discuss the relations between the di-photon signature and other potential signatures in the WW , ZZ and $Z\gamma$ final states. In Section III we provide prospects for probing these accompanying final states during the 13 TeV Run of LHC in terms of required integrated luminosity \mathcal{L} . In

Section IV we discuss the range of validity of our analysis, particularly regarding a possible mixing of S with the SM Higgs. Finally, we conclude in Section V.

II. S DECAYS BEYOND $\gamma\gamma$

In the following, I assume that the loop-induced decay $S \rightarrow \gamma\gamma$ is dominantly mediated by just one new particle species χ with certain EW quantum numbers, and that S is (mostly) an EW singlet, such that potential tree-level decays of S into WW and ZZ are suppressed compared to the corresponding loop-induced ones (I discuss the range of validity of this approximation in Section IV). Then, the ratio of S -mediated di-photon production to that of S -mediated WW , ZZ and $Z\gamma$ production is independent of the coupling $\lambda_{S\chi}$ between S and χ , its mass m_χ or the bosonic/fermionic nature of χ : The ratios R_{VV} depend solely on the EW quantum numbers of χ , and as such they constitute an ideal observable for probing the $SU(2)_L \times U(1)_Y$ properties of χ . The various ratios R_{VV} read, in the limit $m_S \gg m_W, m_Z$ (see *e.g.* [9–11])

$$R_{Z\gamma} = \frac{2 \left(\frac{c_W}{s_W} - \kappa \frac{s_W}{c_W} \right)^2}{(1 + \kappa)^2} \quad (1)$$

$$R_{ZZ} = \frac{\left(\frac{c_W^2}{s_W^2} + \kappa \frac{s_W^2}{c_W^2} \right)^2}{(1 + \kappa)^2} \quad (2)$$

$$R_{WW} = \frac{2}{s_W^4 (1 + \kappa)^2} \quad (3)$$

with s_W (c_W) being the sine (cosine) of the Weinberg angle. As (1)-(3) show, all three ratios R_{VV} are fully controlled by the one parameter κ if S is an un-mixed $SU(2)_L \times U(1)_Y$ gauge singlet¹. The value of κ is given by

$$\kappa = \frac{12 Y^2}{(N - 1)(N + 1)} \quad (4)$$

¹ In contrast, if S contains an admixture of the SM Higgs doublet (or another new scalar, transforming non-trivially under $SU(2)_L$ [12]), then tree-level decays into WW and ZZ introduce an extra parameter dependence [10].

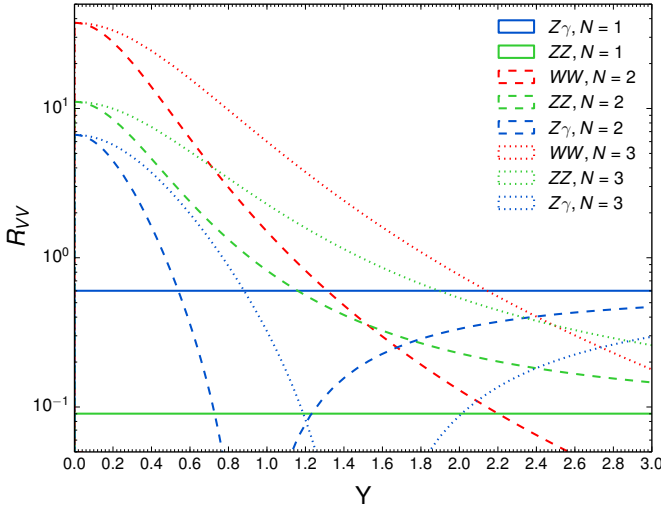


FIG. 1. R_{VV} (with $VV = Z\gamma, ZZ, WW$) as a function of Y for $N = 1, 2, 3$ (for $N = 1$, $Y > 0$ is implied).

where Y is the hypercharge of χ and $N = 1, 2, 3, 4, \dots$ denotes its $SU(2)_L$ representation (1 = singlet, 2 = doublet, 3 = triplet...). In Figure 1 we show the values of R_{VV} as a function of Y for $N = 1, 2, 3$. The values of all $R_{Z\gamma}$, R_{ZZ} and R_{WW} are maximized for $Y = 0$ ($\kappa = 0$, with χ being a pure $SU(2)_L$ state), while for χ being a pure $U(1)_Y$ state ($N = 1$, $\kappa = \infty$), both R_{ZZ} and R_{WW} reach their minimum values $R_{ZZ} = 0.0902$ and $R_{WW} = 0$, while $R_{Z\gamma} = 0.6008$ (the ratios are independent of the value of Y , but $Y > 0$ is implied). As seen from (1), $R_{Z\gamma}$ reaches its minimum $R_{Z\gamma} = 0$ for $N > 1$ and $Y^2 = c_W^2(N-1)(N+1)/(12s_W^2)$. We also note that while for $\kappa = 0$ we have $R_{WW} > R_{ZZ} > 1$, as κ increases there is a turning point above which $1 > R_{ZZ} > R_{WW}$, which occurs for $\kappa > c_W^2(\sqrt{2} - c_W^2)/s_W^4$.

We stress that, as is apparent from the relations (1)-(4), for $N > 1$ only a combination of N and Y can be accessed by the measurement of the ratios R_{VV} , but not the $SU(2)_L$ representation of χ alone. However, such measurement of the ratios does provide disentangling power among $N = 1$, $N > 1$ with $Y > 0$, and $N > 1$ with $Y = 0$. In the next Section we analyze the prospects for LHC 13 TeV (as well as the constraints from LHC 8 TeV) in this respect.

III. PROSPECTS FOR LHC 13 TeV

In order to analyze the LHC 13 TeV prospects of probing the di-photon resonance S accompanying decays $S \rightarrow Z\gamma$, $S \rightarrow ZZ$ and $S \rightarrow WW$, and provide a robust estimate of the integrated luminosity \mathcal{L} needed to exclude at 95% C.L. the presence of these new decay modes for different $SU(2)_L$ representations and values of the $U(1)_Y$ hypercharge Y , the di-photon cross section $\sigma(pp \rightarrow S \rightarrow \gamma\gamma)$ required to fit the ATLAS and CMS 13 TeV data is needed. Under the assumption of a narrow

width² (NW) for S , the central value (CV) and the lowest value allowed at 95% C.L. for the di-photon cross section from a fit to the 13 TeV ATLAS 3.2 fb^{-1} of data [13] are respectively given by

$$\sigma_{\gamma\gamma\text{ATLAS}}^{\text{NW-CV}} \simeq 7.5 \text{ fb} \quad , \quad \sigma_{\gamma\gamma\text{ATLAS}}^{\text{NW-95\%}} \simeq 3.1 \text{ fb}. \quad (5)$$

Similarly, the respective di-photon cross sections from the 13 TeV CMS di-photon 3.3 fb^{-1} data fit [4] are

$$\sigma_{\gamma\gamma\text{CMS}}^{\text{NW-CV}} = 4.87 \text{ fb} \quad , \quad \sigma_{\gamma\gamma\text{CMS}}^{\text{NW-95\%}} = 0.91 \text{ fb}. \quad (6)$$

In contrast, for a wide resonance² (LW), with $\Gamma_S \sim 45$ GeV, the above di-photon cross sections read

$$\sigma_{\gamma\gamma\text{ATLAS}}^{\text{LW-CV}} \simeq 13 \text{ fb} \quad , \quad \sigma_{\gamma\gamma\text{ATLAS}}^{\text{LW-95\%}} \simeq 6.5 \text{ fb}, \quad (7)$$

$$\sigma_{\gamma\gamma\text{CMS}}^{\text{LW-CV}} \simeq 4.2 \text{ fb} \quad , \quad \sigma_{\gamma\gamma\text{CMS}}^{\text{LW-95\%}} \simeq 0.8 \text{ fb}. \quad (8)$$

The ATLAS cross sections in (7) are again obtained from [13], while the CMS ones are obtained via a proper rescaling of the NW cross sections in (6) using the respective significances from the $m_{\gamma\gamma} = 750$ GeV p -values for NW ($\Gamma_S/m_S = 0.00014$) and LW ($\Gamma_S/m_S = 0.056$) from [4]. We remark that our choice of di-photon signal cross section benchmarks (CV and lowest value allowed at 95% C.L.) is motivated by the fact that significantly higher values (in particular the highest allowed value at 95% C.L. for $\sigma_{\gamma\gamma}$ from 13 TeV LHC data) are excluded at more than 95% C.L. by LHC 8 TeV CMS di-photon data [14].

Both ATLAS and CMS have very recently performed searches for heavy spin-0 resonances decaying to $Z\gamma$ [15, 16], ZZ [17, 18] and WW [19] at 13 TeV, providing 95% C.L. upper bounds on the respective cross sections. Focusing on the most stringent limits for each channel³, in combination with the required range of di-photon cross sections (5)-(8) these allow to constrain the value of the various ratios R_{VV} in (1). Since the improvement on the 13 TeV bounds is expected to scale simply as $\sim \sqrt{\mathcal{L}}$ in the future (as the current bounds are already obtained from 13 TeV data, the signal and background efficiencies of these analyses are expected not to change significantly as more data is collected), it is then possible to obtain a fairly robust estimate of the required amount of integrated luminosity \mathcal{L} to exclude at 95% C.L. the presence of the decay modes $S \rightarrow Z\gamma, ZZ, WW$ for different

² The criterium for NW *vs* LW refers to experimental mass resolution. We note that for LW with $\Gamma_S \sim 45$ GeV, the ratio $\Gamma_S/m_S \sim 0.05$, so that S may still be considered a narrow resonance in the broad sense.

³ The ATLAS bounds are obtained with 3.2 fb^{-1} of data, *vs* the CMS 2.7 fb^{-1} (2.3 fb^{-1}) of data in the $Z\gamma$ (ZZ) analysis. The ATLAS constraints are generically stronger, with the sole exception of the LW scenario for $Z\gamma$ and ZZ , for which an ATLAS analysis does not exist, while a CMS one does.

$SU(2)_L$ representations and values of the $U(1)_Y$ hypercharge Y . As discussed at the end of Section II, there are three qualitatively distinct scenarios to be probed: The pure $U(1)_Y$ scenario, the pure $SU(2)_L$ scenario and the

case of χ being charged under both. These three scenarios can be fully explored then by considering the case of χ as an $SU(2)_L$ singlet with $Y > 0$ and the case of χ as an $SU(2)_L$ doublet with $Y \geq 0$.

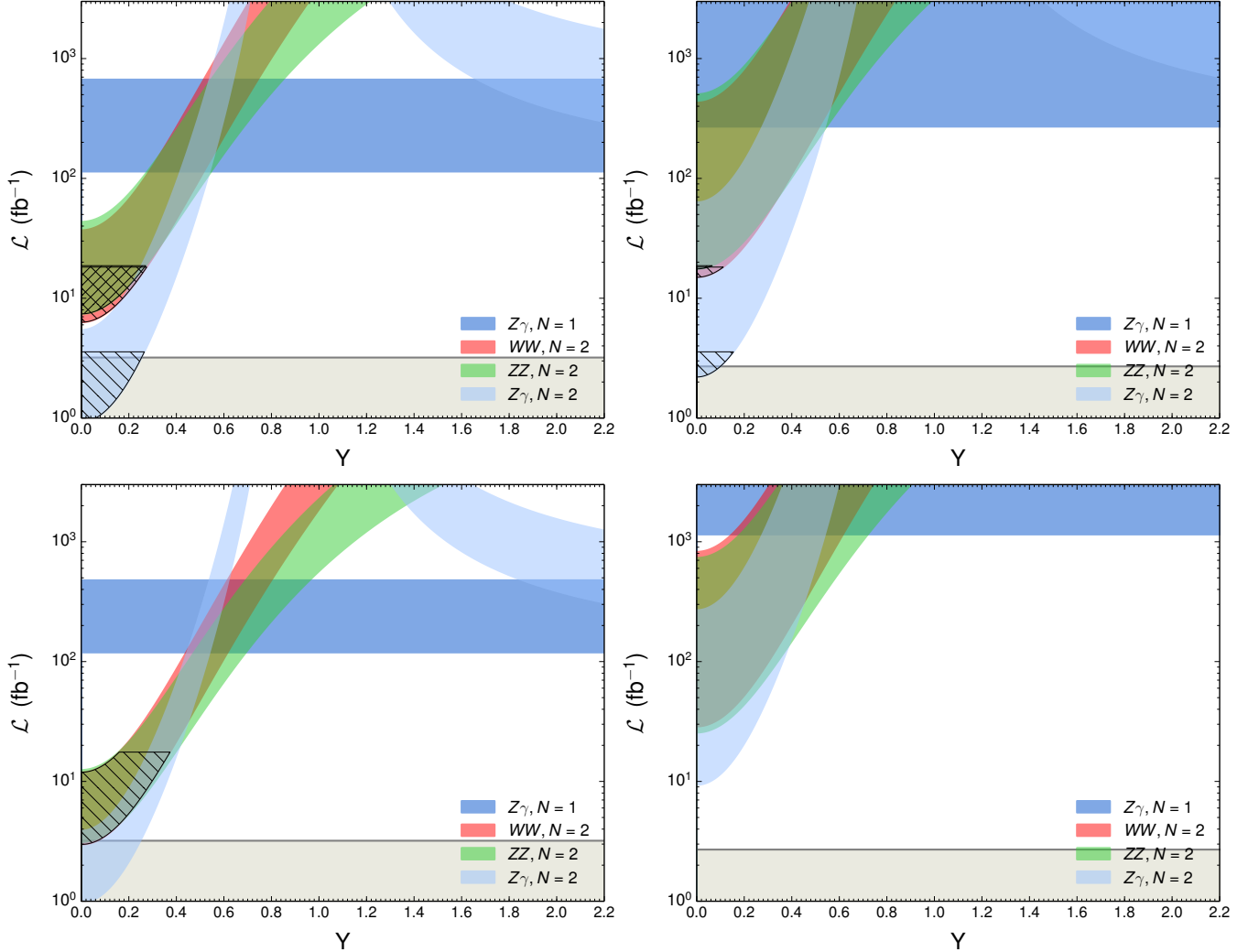


FIG. 2. Integrated luminosity \mathcal{L} (in fb^{-1}) needed to exclude at 95% C.L. the presence of the decays $S \rightarrow Z\gamma$ (blue), $S \rightarrow ZZ$ (green) and $S \rightarrow WW$ (red), for an $SU(2)_L$ singlet χ ($N = 1$) and $SU(2)_L$ doublet χ ($N = 2$), as a function of the hypercharge Y of χ (for $N = 1$, $Y > 0$ is implied). *Top*: NW scenario, assuming the di-photon production cross section $\sigma(pp \rightarrow S \rightarrow \gamma\gamma)$ range favoured respectively by ATLAS (left), given in (5), and by CMS (right), given in (6). *Bottom*: LW scenario, assuming the di-photon production cross section $\sigma(pp \rightarrow S \rightarrow \gamma\gamma)$ range favoured respectively by ATLAS (left), given in (7), and by CMS (right), given in (8). Dashed areas show the exclusion regions from LHC 8 TeV data (see text for details). The shaded light-grey region indicates the value of \mathcal{L} from current 13 TeV searches.

The results are shown on Figure 2-*Top* for the case of NW assuming the di-photon production cross section ranges favoured respectively by ATLAS (left), given in (5), and by CMS (right), given in (6). Similarly, Figure 2-*Bottom* shows the results for the LW scenario, assuming respectively the di-photon production cross section ranges favoured by ATLAS (left), given in (7), and by CMS (right), given in (8).

For χ being an $SU(2)_L$ singlet ($N = 1$), the WW decay mode is absent, while the ZZ mode is beyond the LHC reach with end-of-lifetime integrated luminosity $\mathcal{L} = 3000 \text{ fb}^{-1}$ both in the NW and LW scenarios. In contrast, the $Z\gamma$ decay mode would be within 13 TeV LHC reach with $\mathcal{L} = 100 - 500 \text{ fb}^{-1}$ for the di-photon cross section range favoured by ATLAS (both for NW and LW). We however note that for the di-photon cross

section range favoured by CMS, the required \mathcal{L} to probe the $Z\gamma$ channel increases significantly. This is particularly so for the LW scenario, as the local significance of the potential di-photon signal at $m_{\gamma\gamma} = 750$ GeV in the 13 TeV CMS data decreases from $N_\sigma \sim 2.87$ for NW to $N_\sigma \sim 2.52$ for the LW scenario [4]. As a result of the above discussion, the $N = 1$ case may be excluded by probing the WW and/or ZZ decays modes of S at the 13 TeV LHC, as well as by failing to observe the $S \rightarrow Z\gamma$ decay with $\mathcal{L} \sim \mathcal{O}(1000) \text{ fb}^{-1}$ (particularly if more precise measurements of the di-photon cross section agree with the range currently favoured by ATLAS data).

For $N > 1$ and $Y > 0$, a di-photon cross section in the range favoured by ATLAS data would strongly suggest the existence of another gauge boson decay mode of S within LHC reach, both for NW and LW, as shown in Figure 2 (Left). These new channels would be $S \rightarrow ZZ$ and $S \rightarrow WW$ for $1 \lesssim \kappa \lesssim 6$ and an integrated luminosity $\mathcal{L} \gtrsim 30 \text{ fb}^{-1}$, while for $\kappa \gtrsim 6$ the $S \rightarrow Z\gamma$ decay mode would be only one observed at LHC, which would at least need $\mathcal{L} \sim \mathcal{O}(100) \text{ fb}^{-1}$. For $\kappa \lesssim 1$, Figure 2 shows that all three decay modes $S \rightarrow Z\gamma$, $S \rightarrow ZZ$ and $S \rightarrow WW$ would be accessible, with $S \rightarrow Z\gamma$ most likely being the first channel to be discovered.

Finally, for $N > 1$ and $Y = 0$ ($\kappa = 0$), Figure 2 shows that 13 TeV ATLAS and CMS $Z\gamma$ searches already strongly constrain this scenario with $\mathcal{L} \sim 3 \text{ fb}^{-1}$, with the ATLAS and CMS favoured 13 TeV NW-CV di-photon cross sections being excluded at more than 95% C.L., as well as the ATLAS favoured 13 TeV LW-CV di-photon cross section.

LHC 8 TeV ATLAS and CMS searches for spin-0 resonances decaying to $Z\gamma$ [20], WW [21, 23] and ZZ [22, 23] also yield strong constraints on small values of κ . As opposed to the 13 TeV constraints discussed above, in order to derive limits on R_{VV} from 8 TeV data we need to assume a specific production mechanism for S at the LHC, as the ratio $R_\sigma = \sigma_{13 \text{ TeV}}(pp \rightarrow S)/\sigma_{8 \text{ TeV}}(pp \rightarrow S)$ varies for different production mechanisms (being dependent on the parton luminosity evolution from 8 TeV to 13 TeV). In the following we assume gluon fusion production of S , for which $R_\sigma \sim 4.7$ (for $m_S = 750$ GeV). For a NW scenario, the 95% C.L. limits from 8 TeV searches on the corresponding 13 TeV cross sections are $\sigma(pp \rightarrow S \rightarrow Z\gamma) < 25.5 \text{ fb}$ [20], $\sigma(pp \rightarrow S \rightarrow WW) < 165 \text{ fb}$ [21] and $\sigma(pp \rightarrow S \rightarrow ZZ) < 52 \text{ fb}$ [22]. For a LW scenario, the only available analysis is that of [21], yielding a 95% C.L. limit on the corresponding 13 TeV cross section of $\sigma(pp \rightarrow S \rightarrow WW) < 201 \text{ fb}$. All these limits are shown in Figure 2 as dashed regions. As is apparent from Figure 2, the 8 TeV limits exclude the range of di-photon cross sections favoured by 13 TeV ATLAS data in the LW scenario at more than 95% C.L. for $\kappa < 0.0085$. The ranges of di-photon cross sections favoured by 13 TeV ATLAS/CMS data in the NW scenario are also severely constrained.

We note that a direct consequence of our analysis is that, would the 750 GeV resonance be observed in the WW or ZZ channels with an integrated luminosity $\mathcal{L} \lesssim 30 \text{ fb}^{-1}$ and without the prior/simultaneous observation of the corresponding $Z\gamma$ signature, such observation would not be possible to accommodate within the present analysis, which would indicate that S is not a pure $SU(2)_L$ singlet. We comment on this issue in the next Section.

IV. HIGGS-SINGLET MIXING

Let us now discuss the EW nature of S itself, and its impact on the present analysis. First, we note that S could be a neutral state from an $SU(2)_L$ multiplet. However, if S is part of a doublet, *e.g.* as in a Two-Higgs-Doublet model, the alignment limit [24] has to be invoked and even in this case several species of new vector-like fermion states χ with different $SU(2)_L \times U(1)_Y$ quantum numbers are needed (see *e.g.* [11]), leading to a rather baroque scenario. Accommodating the di-photon signature with higher $SU(2)_L$ representations generically fails to achieve the required suppression of the tree-level decays $S \rightarrow WW, ZZ$ [25] to comply with bounds from ATLAS and CMS searches at LHC 8 TeV. The above issues then favour S being predominantly an EW singlet. If it is a pseudoscalar, then mixing of S with the SM Higgs is automatically avoided and the analysis carried out in this work fully applies. On the other hand, if S is a scalar, then mixing of S with the SM Higgs will occur (even if not present at tree-level, it will always occur at some loop order), leading to tree-level decays $S \rightarrow WW, ZZ$ which could potentially modify the results of the present analysis. We now quantify the range of validity of our analysis in the presence of Higgs-singlet mixing, parametrized here by $\sin \theta \equiv s_\theta$, and then discuss the experimental constraints on the value of such mixing.

Let us consider for simplicity $VV = WW$, and χ to be an n -tuple of vector-like fermions, whose Yukawa-type coupling to S reads

$$\lambda_{S\chi} S \bar{\chi} \chi. \quad (9)$$

Our analysis from Sections II and III is strictly valid in the limit $s_\theta \rightarrow 0$. In this limit, the partial decay width Γ_{WW} induced at 1-loop by (9) (implicitly assuming $N > 1$) is given by (see *e.g.* [11])

$$\begin{aligned} \Gamma_{WW}^{\text{loop}} &\simeq \frac{2\alpha_{\text{EM}}^2 m_S}{144^2 \pi^3 s_W^4} n^2 \lambda_{S\chi}^2 \mathcal{A}_{\frac{1}{2}}^2(\tau_\chi) \\ &\times [N(N-1)(N+1)]^2 \end{aligned} \quad (10)$$

with n also accounting for potential colour degrees of freedom, $\tau_\chi = m_S^2/(4m_\chi^2) < 1$, and $\mathcal{A}_{\frac{1}{2}}(x)$ being a loop function which can be found *e.g.* in [26].

In the presence of Higgs-singlet mixing $s_\theta \neq 0$, but now in the absence of new states χ which would yield loop-induced contributions to $S \rightarrow WW$, the decay is entirely due to Higgs-singlet mixing, with a partial decay width given by [27]

$$\Gamma_{WW}^{\text{tree}} = s_\theta^2 \times \Gamma_{WW}^{\text{SM}}(m_S) = s_\theta^2 \times 145 \text{ GeV}. \quad (11)$$

The consistency of our analysis requires $\Gamma_{WW}^{\text{tree}}/\Gamma_{WW}^{\text{loop}} \lesssim 1$, which leads to

$$|s_\theta| \lesssim 1.3 \times 10^{-4} \left[n \lambda_{S\chi} \mathcal{A}_{\frac{1}{2}}(\tau_\chi) N(N-1)(N+1) \right]. \quad (12)$$

A similar bound may be obtained (now involving the value of the hypercharge Y) for $VV = ZZ$. Since models fitting the di-photon excess typically require the bracketed term in (12) to be $\sim \mathcal{O}(100)$ [28], this yields an approximate bound $|s_\theta| \lesssim 10^{-2}$.

The above discussion implies that for a pseudoscalar S our results are generically robust. For a scalar S , our analysis fully applies if the Higgs-singlet mixing occurs at 1-loop or higher (since then $|s_\theta| < (16\pi^2)^{-1}$ is expected) whereas for tree-level Higgs-singlet mixing a high degree of tuning is required. This also highlights the fact that an SM+ S EFT analysis of the di-photon anomaly, with S being an $SU(2)_L \times U(1)_Y$ singlet scalar, requires the inclusion of Higgs-singlet mixing effects [10, 29, 30].

Turning to the analysis of experimental bounds on the mixing, we first note that the amount of mixing s_θ is severely constrained by measurements of EW precision observables (EWPO). We can safely neglect the impact of the new states χ on EWPO for $m_\chi > 375 \text{ GeV}$ (as the region of parameter space where they could be relevant is ruled out by Drell-Yan measurements at LHC 8 TeV [7]), and then EWPO directly constrain the presence of Higgs-singlet mixing. The shift on any oblique parameter $\mathcal{O} = S, T, U$ due to the Higgs-singlet mixing can be written entirely in terms of the SM Higgs contribution to that parameter, $\mathcal{O}^{\text{SM}}(m)$, where m is either m_h or m_S

$$\begin{aligned} \Delta\mathcal{O} &= (c_\theta^2 - 1)\mathcal{O}^{\text{SM}}(m_h) + s_\theta^2 \mathcal{O}^{\text{SM}}(m_S) \\ &= s_\theta^2 (\mathcal{O}^{\text{SM}}(m_S) - \mathcal{O}^{\text{SM}}(m_h)), \end{aligned} \quad (13)$$

Taking the best-fit values for the shifts $\Delta\mathcal{O}$ from the latest EW fit to the SM by the Gfitter group [31] and performing a χ^2 fit to these data (for details, see [32]) leads to the bound $|s_\theta| < 0.24$.

Another powerful source of constraints on the value of s_θ comes from LHC 8 TeV ATLAS and CMS searches for high-mass spin-0 resonances decaying to WW and ZZ [21–23]. We note that these limits, discussed in the previous Section, depend mildly on the amount of mixing (as it influences the width of S), as well as on the LHC production mechanism for S and the choice of favoured range for the 13 TeV di-photon cross section (for ATLAS or CMS). We consider gluon fusion production for

S , and neglect for simplicity the 1-loop contributions to the decay amplitudes for $S \rightarrow WW$ and $S \rightarrow ZZ$, in order to disregard the possible effect of interplay between the tree-level and 1-loop contributions to the amplitudes (see [30] for a recent discussion of these effects). We can then give an estimate of the upper bound on $\Gamma_{VV}^{\text{tree}}/\Gamma_{\gamma\gamma}$ as a bound on R_{VV} from 8 TeV searches (see Figure 2). For $V = W$, $\Gamma_{WW}^{\text{tree}}$ is given by (11), while for $V = Z$, $\Gamma_{ZZ}^{\text{tree}} = s_\theta^2 \times 72 \text{ GeV}$ [27]. The di-photon partial width of S is given by

$$\begin{aligned} \Gamma_{\gamma\gamma} &= \frac{\alpha_{\text{EM}}^2 m_S}{144^2 \pi^3} n^2 \lambda_{S\chi}^2 \mathcal{A}_{\frac{1}{2}}^2(\tau_\chi) \\ &\times N^2 [12 Y^2 + (N-1)(N+1)]^2. \end{aligned} \quad (14)$$

Bearing in mind that fitting the di-photon excess requires $n \lambda_{S\chi} \mathcal{A}_{\frac{1}{2}}(\tau_\chi) N [12 Y^2 + (N-1)(N+1)] \sim \mathcal{O}(100)$, and considering for a conservative estimate the lower edge of the ATLAS and CMS favoured ranges for the di-photon signal cross section, we obtain a rough bound $|s_\theta| \lesssim 0.03$, in good agreement with [30]. The fact that this bound is of the same order as the bound on $|s_\theta|$ for the consistency of our analysis, given by (12), highlights that current limits on R_{VV} from 8 TeV data are of similar order as the values of R_{VV} for a pure $SU(2)_L$ singlet S decaying to SM gauge bosons via loops of χ particles⁴ with $SU(2)_L \times U(1)_Y$ quantum numbers such that $\kappa \ll 1$, as discussed in Section II.

V. CONCLUSIONS

The existence of a 750 GeV di-photon spin-0 resonance S , if confirmed by upcoming LHC data, would have profound implications for physics beyond the SM. Among them would be the additional presence of new degrees of freedom χ coupled to S and electromagnetically charged. Unravelling the properties of these new states would then become a key task for LHC. In this work I have discussed a powerful probe of the $SU(2)_L \times U(1)_Y$ quantum numbers of these new states χ , through measurements of the ratios R_{VV} between the cross sections $pp \rightarrow S \rightarrow VV$ with $VV = Z\gamma, ZZ, WW$ and the di-photon cross section measured by ATLAS and CMS. These probes are independent of the bosonic/fermionic nature of the new states χ , their mass and coupling to S . I have provided robust estimates of the amount of LHC integrated luminosity \mathcal{L} required to explore various possible scenarios, showing in particular that LHC has the capability to disentangle the pure $SU(2)_L$ case, the pure $U(1)_Y$ case and the case when χ transform under both symmetries, from each other. This would provide

⁴ This also stresses the importance of accounting for the interplay between tree-level and 1-loop contributions to the decay amplitude, in the presence of Higgs-singlet mixing, for a precise bound on s_θ [30].

very useful information on the underlying theory beyond the SM, as well as on the strategy to search for these new states directly at the LHC and beyond. as well as on the strategy to search for these new states directly at the LHC and beyond.

Acknowledgements

I want to thank Tilman Plehn, Veronica Sanz and Ken Mimasu for useful discussions and comments on the manuscript, as well as the Mitchell Institute for Theoretical Physics from Texas A&M University and the Institute for Theoretical Physics from Heidelberg University, for their kind hospitality while this work was being performed. J.M.N. is supported by the People Programme (Marie Curie Actions) of the European Union Seventh Framework Programme (FP7/2007-2013) under REA grant agreement PIEF-GA-2013-625809.

-
- [1] Tech. Rep. ATLAS-CONF-2015-081, CERN, Geneva, Dec, 2015
 - [2] The ATLAS collaboration, ATLAS-CONF-2016-018.
 - [3] CMS Collaboration [CMS Collaboration], collisions at 13TeV, CMS-PAS-EXO-15-004.
 - [4] CMS Collaboration [CMS Collaboration], CMS-PAS-EXO-16-018.
 - [5] S. Knapen, T. Melia, M. Papucci and K. Zurek, Phys. Rev. D **93** (2016) no.7, 075020 [arXiv:1512.04928 [hep-ph]].
 - [6] J. Ellis, S. A. R. Ellis, J. Quevillon, V. Sanz and T. You, JHEP **1603** (2016) 176 [arXiv:1512.05327 [hep-ph]].
 - [7] C. Gross, O. Lebedev and J. M. No, arXiv:1602.03877 [hep-ph].
 - [8] F. Goertz, A. Katz, M. Son and A. Urbano, arXiv:1602.04801 [hep-ph].
 - [9] I. Low and J. Lykken, arXiv:1512.09089 [hep-ph].
 - [10] R. Franceschini, G. F. Giudice, J. F. Kamenik, M. McCullough, F. Riva, A. Strumia and R. Torre, arXiv:1604.06446 [hep-ph].
 - [11] W. Altmannshofer, J. Galloway, S. Gori, A. L. Kagan, A. Martin and J. Zupan, arXiv:1512.07616 [hep-ph].
 - [12] K. Howe, S. Knapen and D. J. Robinson, arXiv:1603.08932 [hep-ph].
 - [13] M. R. Buckley, arXiv:1601.04751 [hep-ph].
 - [14] V. Khachatryan *et al.* [CMS Collaboration], Phys. Lett. B **750** (2015) 494 [arXiv:1506.02301 [hep-ex]].
 - [15] The ATLAS collaboration, ATLAS-CONF-2016-010.
 - [16] CMS Collaboration [CMS Collaboration], CMS-PAS-EXO-16-019.
 - [17] The ATLAS collaboration, ATLAS-CONF-2016-012.
 - [18] CMS Collaboration [CMS Collaboration], CMS-PAS-HIG-16-001.
 - [19] The ATLAS collaboration, ATLAS-CONF-2016-021.
 - [20] CMS Collaboration [CMS Collaboration], CMS-PAS-HIG-16-014.
 - [21] G. Aad *et al.* [ATLAS Collaboration], JHEP **1601** (2016) 032 [arXiv:1509.00389 [hep-ex]].
 - [22] G. Aad *et al.* [ATLAS Collaboration], Eur. Phys. J. C **76** (2016) no.1, 45 [arXiv:1507.05930 [hep-ex]].
 - [23] V. Khachatryan *et al.* [CMS Collaboration], JHEP **1510** (2015) 144 [arXiv:1504.00936 [hep-ex]].
 - [24] J. F. Gunion and H. E. Haber, Phys. Rev. D **67** (2003) 075019 [hep-ph/0207010].
 - [25] C. W. Chiang and A. L. Kuo, arXiv:1601.06394 [hep-ph].
 - [26] D. Carmi, A. Falkowski, E. Kuflik, T. Volansky and J. Zupan, JHEP **1210** (2012) 196 [arXiv:1207.1718 [hep-ph]].
 - [27] S. Dittmaier *et al.* [LHC Higgs Cross Section Working Group Collaboration], arXiv:1101.0593 [hep-ph].
 - [28] J. M. No, V. Sanz and J. Setford, arXiv:1512.05700 [hep-ph].
 - [29] B. Gripaios and D. Sutherland, arXiv:1604.07365 [hep-ph].
 - [30] S. Dawson and I. M. Lewis, arXiv:1605.04944 [hep-ph].
 - [31] M. Baak *et al.* [Gfitter Group Collaboration], Eur. Phys. J. C **74** (2014) 3046 [arXiv:1407.3792 [hep-ph]].
 - [32] M. Gorbahn, J. M. No and V. Sanz, JHEP **1510** (2015) 036 [arXiv:1502.07352 [hep-ph]].